Chemical Engineering Journal 152 (2009) 212–219

Contents lists available at ScienceDirect

Chemical Engineering Journal

journal homepage: www.elsevier.com/locate/cej

Retention of Cr(VI) and Pb(II) on a loamy sand soil
Kinetics, equilibria and breakthrough

B. Fonseca*, H. Maio, C. Quintelas, A. Teixeira, T. Tavares

IBB-Institute for Biotechnology and Bioengineering, Centre of Biological Engineering, University of Minho, 4710-057 Braga, Portugal

ARTICLE INFO

Article history:
Received 23 December 2008
Received in revised form 8 April 2009
Accepted 16 April 2009

Keywords:
Adsorption equilibria
Breakthrough
pH
Heavy metals
Soil

ABSTRACT

Illegal discharges are of great concern among industry activities, since they occur under uncontrolled conditions. In most cases, effluents are acidic and the concentrations of heavy metals are very high. With this in mind, the main goal of this study was to evaluate the sorption on a soil of two of the most toxic heavy metals, Cr(VI) and Pb(II), in those conditions.

A loamy sand soil was collected in Oporto, Portugal. Batch equilibrium and sorption kinetics were evaluated using both metals solutions, with concentrations ranging from 50 mg L^{-1} to 200 mg L^{-1}, at pH 2 and 5, between 2 h and 288 h.

To evaluate the sorption equilibrium, eight isotherm models were fitted to experimental data. The best adjustments were observed for the Redlich–Peterson and Khan models for the adsorption of chromium ($R^2 = 0.99$), and of lead ($R^2 = 0.99$), respectively. The sorption kinetics was evaluated using three models – Elovich, pseudo first order and an empirical power function. The retention of lead was almost instantaneous and the empirical power function described better the sorption kinetics of chromium ($0.89 < R^2 < 0.99$).

In addition, flow experiments were performed with effluents of both metals (50 mg L^{-1}) at pH 2 and 5, for about 90 h. Results revealed a high retention of chromium and a weak retention of lead, for low pH values. FTIR analyses to the column samples revealed that clay minerals have an important role in the retention of both metals.

1. Introduction

Release of heavy metals into soils, as a result of anthropogenic activities like disposal of industrial effluents and spreading of sewage sludge, has raised the concentration of heavy metals in soils to toxic levels [1–3]. Therefore, the study of sorption processes is of utmost importance to understand how the contaminants are transferred from the liquid phase to the solid phase and retained therein [4,5]. Moreover the understanding of the contamination processes of this particular loamy sand soil is fundamental for the recovery of extensive polluted areas, as this type of soil is very common in industrialized regions.

Chromium and lead are among the most toxic heavy metals present in some industrial effluents, which are sometimes directly discharged in soils. Chromium has been widely used among various industries, such as metal plating and leather tanning. The most stable oxidation states of chromium commonly found in nature are Cr(III) and Cr(VI) [6–9]. While Cr(III) is essential for metabolic processes, Cr(VI) is toxic and carcinogenic. Moreover, as an oxyanion, is highly mobile in soil and water [10–12]. On the other hand, lead has a low mobility and is strongly retained by soil constituents. Lead occurs mainly as a divalent cation – Pb(II) – which, being not essential to plants or animals, is known to be hazardous to health [13,14]. Exogenous sources of lead in soil include fossil fuels, mining and smelting operations, and road runoff water [15,16].

The retention on soils of both metals is controlled mainly by redox reactions, precipitation, nucleation and adsorption/desorption processes [13,17]. These sorption processes are affected by many factors (e.g. organic matter, cationic exchange capacity, pH of soil). Many studies have focused on the sorption of chromium and lead under different experimental conditions, but always at the equilibrium pH of the soil and/or with low concentrations of those metals [1,18–21]. However, acid spills of high contaminated industrial effluents occur sporadically, and a different behavior of those contaminants could be expected.

Therefore, the aim of this study is to evaluate the sorption processes of Cr(VI) and Pb(II) present in acid solutions highly concentrated. Specifically, batch equilibrium experiments to generate sorption isotherms and kinetic data using single metal solutions at initial pH of 2 and 5, were undertaken. In addition, to obtain better and more realistic means of evaluating soil performance at the tested pH values, column experiments were also performed.

---

* Corresponding author. Tel.: +351 253 604 400; fax: +351 253 678 986.
E-mail address: bfonseca@deb.uminho.pt (B. Fonseca).

1385-8947/$ – see front matter © 2009 Elsevier B.V. All rights reserved.
doi:10.1016/j.cej.2009.04.045

The retardation factor – R – was determined by the method used previously by the authors [22]. Batch tests data were analyzed and fitted by eight sorption isotherms – Freundlich, Langmuir, Dubinin–Radushkevich, Temkin, Redlich–Peterson, Khan, Sips and Toth – and three kinetic models – Lagergren, Elovich and empirical power function equation – since some of these models have been successfully used to predict and compare sorption performance of various soils and heavy metals [1–3,13,20,23,24].

FTIR spectra analyses performed on different samples of contaminated soils indicate that clays play an important role in the overall retention process and the presence of surface groups usually responsible for metal ions adsorption was confirmed.

2. Theory

2.1. Sorption kinetics

Lagergren's first order rate equation is the oldest known one describing the adsorption rate based on the adsorption capacity. It assumes that the reaction rate is limited by only one process or mechanism on a single class of sorbing sites and that all sites are of the time dependent type [3,25]:

$$\frac{\mathrm{d}q_t}{\mathrm{d}t} = k_1(q_\mathrm{e} - q_t) \tag{1}$$

Elovich's equation is useful to describe sorption reactions without desorption of products. The adsorption rate decreases with time due to the increased surface coverage [26]:

$$\frac{\mathrm{d}q_t}{\mathrm{d}t} = \alpha \mathrm{e}^{-\beta q_t} \tag{2}$$

In this study the Power Function Equation was also used. Besides its empirical character, this equation provides a good method to compare experimental results [1,5]:

$$q_t = kt^{\nu} \tag{3}$$

In these equations t is the contact time (h); q_t is the amount of metal sorbed per unit mass of soil at time t (mg kg^{-1}); k_1 is the first order rate constant (h^{-1}); q_e is the amount of metal sorbed per unit mass of soil at equilibrium (mg kg^{-1}); α is the initial adsorption rate (mg kg^{-1} h^{-1}) and β is the desorption constant (kg mg^{-1}) of Elovich equation; k (mg kg^{-1} h$^{-\nu}$) and ν are adjustment parameters of the Power Function Equation.

2.2. Equilibrium models

Four isotherm models with two adjustable parameters and four models with three adjustable parameters were used to describe the experimental data.

2.2.1. Two parameters isotherms

Freundlich equation assumes that the stronger binding sites are occupied first and that the binding strength decreases with the increasing degree of site occupation. It is described as:

$$q_\mathrm{e} = k_\mathrm{F} C_\mathrm{e}^{1/n} \tag{4}$$

where q_e is defined earlier, C_e is the concentration of metal in the solution at equilibrium (mg L^{-1}); k_F is the distribution coefficient (L$^{1/n}$ mg kg^{-1} mg$^{-1/n}$) and n is a correction factor [5,27].

A form of Langmuir isotherm is commonly applied to adsorption of heavy metal ions onto soil. It assumes that adsorption occurs until the solid surface is completely covered by a layer of molecules/atoms:

$$q_\mathrm{e} = \frac{q_\mathrm{max} b_\mathrm{L} C_\mathrm{e}}{1 + b_\mathrm{L} C_\mathrm{e}} \tag{5}$$

where q_max is the maximum amount of metal that can be adsorbed (mg kg^{-1}) and b_L is a constant related to the binding strength (L mg^{-1}) [5,28].Dubinin–Radushkevich equation is used to describe systems where the dispersion forces are the dominant component of the adsorption interaction:

$$q_\mathrm{e} = q_\mathrm{D} \mathrm{e}^{-B_\mathrm{D}[RT \ln(1+(1/C_\mathrm{e}))]^2} \tag{6}$$

where q_D is the maximum adsorption capacity (mg kg^{-1}); B_D is the activity coefficient (mol^2 J^{-2}) related to mean sorption energy – E – (J mol^{-1}), which may be calculated by [29–31]:

$$E = \frac{1}{\sqrt{2B_\mathrm{D}}} \tag{7}$$

The Temkin isotherm considers that the heat of adsorption of all the molecules on the layer decreases linearly with coverage:

$$q_\mathrm{e} = \frac{RT}{b_\mathrm{Te}} \ln(a_\mathrm{Te} C_\mathrm{e}) \tag{8}$$

where R is the gas constant (J mol^{-1} K^{-1}), T is the absolute temperature (K), b_Te is the constant related to the heat of sorption (J mol^{-1}) and a_Te is the Temkin isotherm constant (L mg^{-1}) [30,32].

2.2.2. Three parameters isotherms

The Redlich–Peterson equation was proposed to improve the fit by the Langmuir or the Freundlich equation:

$$q_\mathrm{e} = \frac{k_\mathrm{RP} C_\mathrm{e}}{1 + a_\mathrm{RP} {C_\mathrm{e}}^{\beta_\mathrm{RP}}} \tag{9}$$

where k_RP is the Redlich–Peterson model isotherm constant (L kg^{-1}), a_RP is the model constant (L$^{\beta_\mathrm{RP}}$ mg$^{-\beta_\mathrm{RP}}$) and β_RP is the model exponent [33].

Khan proposed a simple expression for a generalized model for a single solute that can cover extreme cases of Langmuir and Freundlich type isotherms:

$$q_\mathrm{e} = \frac{q_\mathrm{max} b_\mathrm{K} C_\mathrm{e}}{(1 + b_\mathrm{K} C_\mathrm{e})^{a_\mathrm{K}}} \tag{10}$$

where q_max was defined earlier, b_K is the Khan model constant (L mg^{-1}) and a_K is the model exponent [34].

The Sips equation predicts a monolayer sorption capacity for high sorbate concentrations and reduces to Freundlich equation for lower sorbate concentrations:

$$q_\mathrm{e} = \frac{k_\mathrm{S} {C_\mathrm{e}}^{\beta_\mathrm{S}}}{1 + a_\mathrm{S} {C_\mathrm{e}}^{\beta_\mathrm{S}}} \tag{11}$$

where k_S is the Sips model isotherm constant (mg L$^{\beta_\mathrm{S}}$ mg$^{-\beta_\mathrm{S}}$ kg^{-1}), a_S is the model constant (L$^{\beta_\mathrm{S}}$ mg$^{-\beta_\mathrm{S}}$) and β_S is the model exponent [30,35].

The Toth's model derived from the potential theory and applies to heterogeneous adsorption:

$$q_\mathrm{e} = \frac{q_\mathrm{max} C_\mathrm{e}}{(k_\mathrm{T} + {C_\mathrm{e}}^{n_\mathrm{T}})^{1/n_\mathrm{T}}} \tag{12}$$

where k_T is the Toth model constant (mg$^{n_\mathrm{T}}$ L$^{-n_\mathrm{T}}$) and n_T is the model exponent [30,36].

3. Material and methods

3.1. Soil characterization

A bulk soil sample was collected in Póvoa de Varzim, Oporto, Portugal at depth of 0–50 cm, near EN 13 road (41°25′15.58″N and 8°45′58.27″O). The soil was air-dried, homogenized and sifted through a 2.0 mm stainless steel sieve.

The Cr and Pb concentrations in soil were determined by flame atomic absorption spectrometry (Varian SpectraAA-400), after microwave (Aurora Instruments MW600) digestion with nitric acid using US EPA method 3051A [37]. Soil pH was determined with 1:1 soil/water suspension. Particle distribution was determined by laser granulometry (Beckman-Coulter mod. LS230), the cationic exchange capacity and exchangeable cations were quantified using ammonium acetate at pH 7 [38] and the Mehlich methods [39], respectively. Organic matter content was determined by the Tinsley method [40]. The major mineral composition was determined by X-ray diffraction analysis (Philips PW3710).

3.2. Batch experiments

Batch experiments with Cr and Pb were performed by adding 20 mL of single-metal solution, to 2 g of soil samples in 50 mL polypropylene tubes. Solutions with varying concentrations were prepared from $PbCl_2$ and $K_2Cr_2O_7$, in 0.01 M $CaCl_2$. The initial pH of each solution was adjusted to a desire value – 2 or 5 – by addition of concentrated HNO_3 (65%) and diluted NaOH (0.1 M). The real concentration of each solution was determined by flame atomic absorption. The concentrations for both metals, varied from about 50 mg L^{-1} to 200 mg L^{-1}. Suspensions were agitated in an orbital mixer at room temperature for different contact lengths of time, at 100 rpm – (1 h, 2 h, 4 h, 8 h, 12 h, 16 h, 24 h and 48 h) for the Pb solutions and (4 h, 8 h, 12 h, 24 h, 48 h, 96 h, 144 h, 192 h, 240 h and 288 h) for the Cr solutions. After shaking, the solutions were centrifuged at 10,000 rpm for 10 min. The supernatants were collected in eppendorfs with 2% (v/v) of HNO_3 after pH measuring, stored at 4 °C and analyzed by flame atomic absorption spectrometry. Proper blanks, without the soil sample, and duplicates, were made for each solution concentration and time. The amount of metal adsorbed on the soil is calculated by:

$$q_t = \frac{(C_i - C_e)V}{W} \qquad (13)$$

where C_e was defined earlier, C_i is the initial concentration of metal in the liquid phase (mg L^{-1}); V is the volume of metal solution (L) and W is the weight of the soil sample (kg).

3.3. Column tests

For the continuous flow experiments, 160 g of soil were manually packed into a column of Perspex (25 cm × 3.2 cm) forming a soil bed with 17 cm and a porosity of about 0.32. Deionised water was initially passed at a slow and steady rate to saturate the column.

Then, 20 litters each of $PbCl_2$ and $K_2Cr_2O_7$ solutions were prepared with 50 mg L^{-1} of Pb or Cr, respectively. The pH was adjusted to values of 2 or 5, with HNO_3 and NaOH. The solutions were passed upwards through the columns via a peristaltic pump ($Q \approx 2.6$ mL min^{-1}) to ensure saturated flow conditions. Samples of the column effluent were collected, acidified after pH measurement, and analyzed by flame atomic absorption spectrometry. All experiments were made in duplicate.

After the assays, soil beds were sliced in three samples that were properly homogenized. Than a sample was digested, with nitric acid, in microwave, according US EPA method 3051A [37] and analyzed by flame atomic absorption spectrometry. Soil samples were also characterized, in duplicate, with transmission FTIR (BOMEM MB104) on KBr pressed pellets. Background correction for atmospheric air was used for each spectrum. The resolution was 4 cm^{-1} with minimum of 10 scans for each spectrum and the range was 500–4000 wavenumbers. Spectra were analyzed by comparing the absorption bands of the samples with known absorption frequencies for different types of bonds.

Table 1
Chemical and physical properties of soil sample from Póvoa de Varzim, Portugal.

Texture (%)	
Clay	2.58
Silt	23.06
Sand	74.36
pH (H_2O)	5.9
Cationic exchange capacity (cmol$_c$ kg^{-1})	12.52
Organic matter content (%)	3.5
Exchangeable cation concentrations (cmol$_c$ kg^{-1})	
[Ca^{2+}]	7.20
[Mg^{2+}]	0.81
[K^+]	0.37
[Na^+]	0.52
Apparent density[a]	
ρ_b (kg m^{-3})	1320
Clay minerals (%)	
Kaolinite	41
Illite	31
Esmectite	18
Interstratified	10
Heavy metals concentration (mg kg^{-1})	
[Cr]	42.5
[Pb]	ND

[a] Disturbed sample.

4. Results and discussion

4.1. Soil characterization

Table 1 resumes the characterization of the studied soil sample. It was classified as an acidic loamy sand soil, with a high content in organic matter. The cationic exchange capacity is low. From the focused metals, only Cr is present in this soil but in a concentration allowed by national legislation (50 mg kg^{-1}). The predominance in the clay minerals belongs to kaolinite, followed by illite, esmectite and interstratified material.

4.2. Batch experiments

4.2.1. Sorption kinetics

Table 2 shows the adjusted parameters of the kinetic equations for experiments with Cr. According to the correlation coefficient values (R^2), better adjustment was achieved with the empirical power function, represented in Fig. 1a and b for each data set. The initial concentration did affect the estimated apparent sorption rate (ν), which increases with the initial metal concentration in liquid phase (Table 2). This is indicative that the rate limiting factor is affected by metal initial concentration [41]. Fig. 1a and b shows that for similar initial concentrations of Cr, lower values of metal adsorbed per mass of soil were obtained for pH 5. Actually, the rate constants of the empirical power function are smaller than those obtained at pH 2 (Table 2). According to Impellitteri et al. [42], soil with pH-dependent charge tends to deprotonate with increasing pH. However, Cr adsorption is favored if surfaces are positively charged, increasing with reduced pH, since the most common species are in the anionic form ($HCrO_4^-$, CrO_4^{2-} and $Cr_2O_7^{2-}$). This may explain the higher rate constants values for pH 2 [10]. In fact, the pH of the liquid phase tends to increase along the batch experiments revealing the protonation of soil surface.

The correlation coefficients obtained for the adjustment of the Elovich equation to Cr adsorption kinetics revealed a good fitting (Table 2). In fact, the graphs of Fig. 1a and b show the typical behavior described by this model. There is a high rate adsorption at the beginning which decreases along time [43]. The initial higher rate

Table 2
Parameters and correlation coefficients (R^2), of the kinetic equations adjusted to experimental data with initial solution of chromium at pH 2 and 5.

pH	C_i (mg L^{-1})[a]	Pseudo first order			Elovich model					Empirical power function				
		k_1	CI[b]	R^2	α	CI	β	CI	R^2	k	CI	ν	CI	R^2
2	75	0.103	0.048	0.862	15.29	7.11	0.008	0.001	0.988	217.6	66.2	0.226	0.061	0.893
	92	0.052	0.024	0.989	12.13	1.90	0.006	0.000	0.992	185.7	36.6	0.285	0.039	0.989
	128	0.035	0.009	0.893	10.34	2.86	0.005	0.001	0.964	146.4	30.1	0.354	0.040	0.993
	154	0.030	0.010	0.908	9.02	2.46	0.005	0.001	0.963	115.6	36.1	0.377	0.061	0.987
	172	0.032	0.011	0.903	9.97	2.17	0.005	0.001	0.977	142.5	28.0	0.364	0.038	0.994
	189	0.025	0.008	0.913	8.17	2.19	0.005	0.001	0.960	94.3	35.4	0.405	0.073	0.985
	204	0.027	0.007	0.939	7.93	2.80	0.006	0.002	0.931	78.6	22.8	0.435	0.056	0.991
5	78	0.010	0.008	0.806	5.73	3.12	0.011	0.004	0.849	36.1	32.6	0.461	0.174	0.935
	98	0.008	0.001	0.963	4.50	1.54	0.008	0.003	0.892	13.7	11.8	0.663	0.161	0.979
	131	0.006	0.002	0.652	6.95	5.65	0.011	0.006	0.826	53.8	69.6	0.388	0.247	0.880

[a] Initial concentration properly corrected.

[b] CI, 95% confidence intervals of the estimated parameters.

of metal sorption has been attributed to adsorption on high affinity surface sites or on sites with higher bonding strength with the metal. Once these sites are exhausted, the uptake may be controlled by diffusion, precipitation and/or sorption reactions on sites with higher activation energy [44].

During the assays on Pb, with the initial solutions at pH 5, precipitation was noticed. In fact, in Fig. 1d it is obvious that the whole Pb was retained in the solid phase. On the other hand, at pH 2, the adsorption occurs rapidly, Fig. 1c. Consequently, the tested models did not adjust the adsorption kinetics of Pb in the same conditions tested for Cr.

4.2.2. *Equilibrium models*

Once more it was not possible to obtain a good fitting with any of the tested isotherm models in the case of Pb adsorption at pH 5. Therefore, Table 3 shows the results obtained with initial solutions of both metals at pH 2. An overall analysis reveals that almost all isotherm equations fit better the experimental data obtained in batch test with Pb, compared to Cr. Besides, among the two parameters models, Langmuir equation presents the best fitting for Pb (Fig. 2), meaning that these cations are strongly adsorbed as a monolayer covering the solid surface. According to this model, Cr shows more affinity to this soil, since the parameter b_L found is higher. However, the tested soil showed a higher maximum adsorption capacity – $q_{\max}$ – for Pb, as it can be seen in Table 3. This can be explained by the hard–soft acid–base principle. The sorption capacity increases with increasing polarizability and ionic radii and decreasing electronegativity, thus decreasing hardness [45]. According to Ghosh and Biswas [46], the global hardness of Pb is lower than the global hardness of Cr, explaining the lower value of the Langmuir constant – $q_{\max}$ – founded for this metal. For Cr, the best fit was obtained with the Dubinin–Radushkevich equation (Fig. 2) and the value obtained for the mean energy sorption is lower than 8 kJ mol^{-1}, which indicates that adsorption is mainly physical due to weak Van der Waals forces [47].

From the three parameter models fitting, the best correlation coefficients were found for Redlich–Peterson isotherm applied to Cr adsorption and for Khan equation applied to Pb(II) adsorption (Table 3). Redlich–Peterson and Khan equations, properly represented in Fig. 2, covers Langmuir and Freundlich isotherms, suggesting the existence of a monolayer strongly adsorbed on the

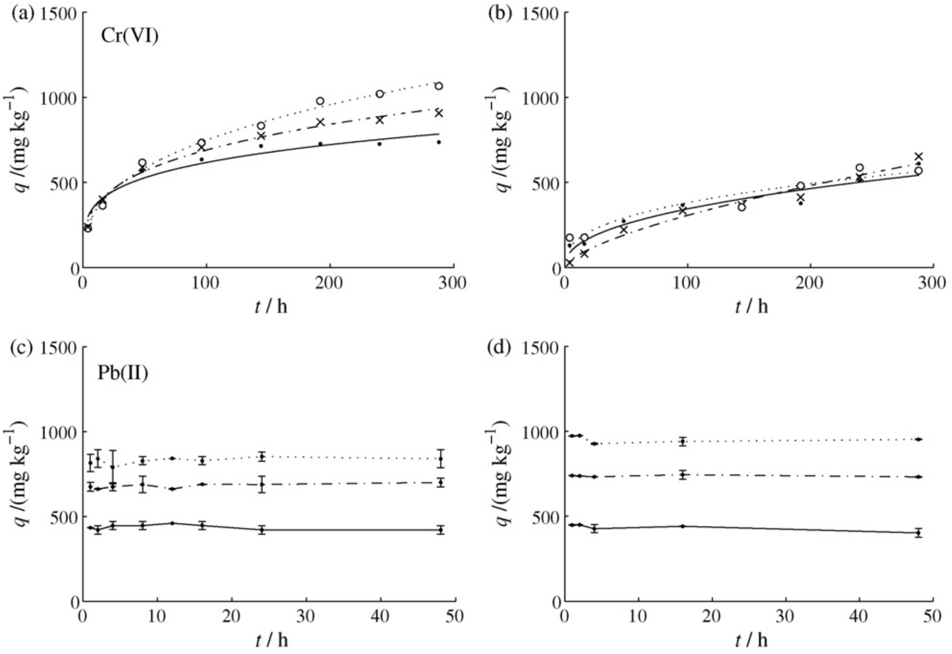

Fig. 1. (a, b) Variation of mass of Cr(VI) adsorbed per mass of soil, for different initial solutions, at pH 2 and 5, respectively (C_1 = 75 mg L^{-1}; C_2 = 92 mg L^{-1}; C_3 = 128 mg L^{-1}). Lines represent the empirical power function, adjusted to each kinetic data; (c, d) variation of mass of Pb(II) adsorbed per mass of soil for different initial solutions, at pH 2 and 5, respectively (C_1 = 78 mg L^{-1}; C_2 = 98 mg L^{-1}; C_3 = 131 mg L^{-1}). The error bars depict the confidence interval for a level of confidence of 95%.

Table 3
Isotherms constants and correlation coefficients (R^2) obtained for the two and three parameter models, for Cr(VI) and Pb(II) sorption onto soil, for initial pH of 2. Confidence intervals determined for a 95% confidence level.

		Cr(VI)	Pb(II)
Two parameter models			
Freundlich	k_F	1078	387.1
	CI	409	202.5
	n	11.33	2.38
	CI	17.46	0.96
	R^2	0.460	0.940
Langmuir	q_{max}	1570	2168
	CI	304	255
	b_L	1.32	0.095
	CI	1.36	0.030
	R^2	0.783	0.990
Dubinin–Radushkevich	q_D	1525	1563
	CI	96	200
	B_D	2.55E−7	4.46E−6
	CI	–	2.39E−6
	E	1400	335
	R^2	0.933	0.929
Temkin	a_{Te}	4443	0.785
	CI	6.448E4	0.366
	b_{Te}	19.84	4.855
	CI	27.78	0.901
	R^2	0.496	0.982
Three parameter models			
Redlich–Peterson	k_{RP}	975	1584
	CI	271	29
	a_{RP}	0.304	0.025
	CI	0.197	0.027
	β_{RP}	1.191	1.285
	CI	0.100	0.247
	R^2	0.987	0.998
Khan	q_{max}	3306	6087
	CI	1334	5365
	a_K	1.262	0.028
	CI	0.190	0.028
	b_K	0.327	1.904
	CI	0.220	1.230
	R^2	0.985	0.999
Sips	k_S	1199	125.6
	CI	1000	98.9
	a_S	0.796	0.067
	CI	0.662	0.044
	β_S	2.360	1.307
	CI	2.183	0.465
	R^2	0.949	0.996
Toth	q_{max}	1496	1786
	CI	134	258
	k_T	23.44	66.35
	CI	128.15	152.86
	n_T	4.05	1.69
	CI	5.90	0.86
	R^2	0.970	0.997

solid surfaces, and, eventually, one or more layers weakly adsorbed due to distance to soil surface [28,30,34].

4.3. Column tests

Variations of Cr and Pb concentration in the effluents [C (mg L^{-1})] relative to the influent [C_i (mg L^{-1})] are shown as breakthrough curves (C/C_i *vs* t) in Fig. 3. As it was mentioned before the Cr oxyanions ($HCrO_4^-$, CrO_4^{2-} and $Cr_2O_7^{2-}$) are weakly sorbed by soils under alkaline to slightly acidic conditions leading to high mobility in the subsurface [11]. Thus, Cr appears in higher concentrations in the leachate of the column fed with dichromate solution at pH 5, Fig. 3a.

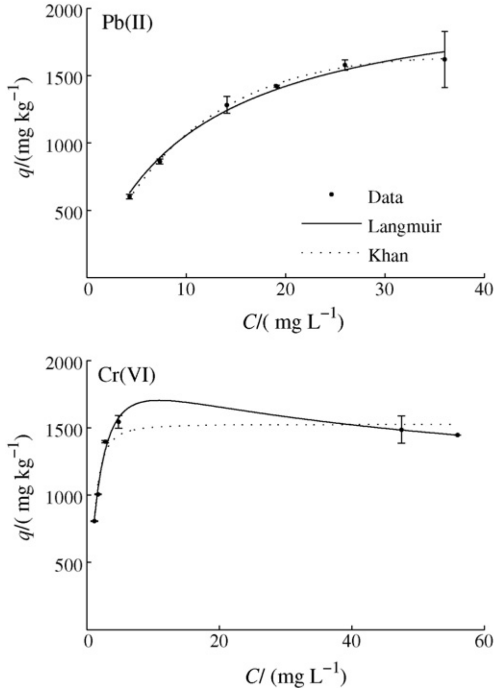

Fig. 2. Sorption isotherms obtained for Cr(VI) and Pb(II) for high equilibrium concentrations. Two parameters models are represented by solid lines and three parameters models by the dash lines. The error bars depict the confidence interval for a level of confidence of 95%.

As it can be seen in Fig. 3c, pH values of the column fed with Cr solution at pH 2 decreased fast. This may be due to the high concentration of protons in this influent that are rapidly sorbed by soil, which has a low buffering capacity, implying a large number of positively charged sites that can retain Cr oxyanions [22]. On the other hand, the lowest concentration of protons in the influent at pH 5 leads to a slower protonation of the solid surfaces. However, these differences can also result from Cr(VI) reduction to Cr(III) that is less mobile due its stronger adsorption and complexation. Other researchers [48,49] showed that organic compounds do not directly reduce Cr(VI) at pH values greater than 2, which can explain the higher retention of Cr in the soil column at pH 2, as it can be seen in Fig. 4 by the higher values of metal concentration in the three soil bed sections. Also, the determination of the retardation factor, by the method used elsewhere by the authors [22], confirmed the higher retention of Cr at pH 2, Table 4.

The breakthrough curve shown in Fig. 3b for the assay with Pb influent at pH 5, indicates that no saturation occurred in this column. On the other hand, at pH 2, Pb showed higher mobility. In fact, the retardation factor obtained for this influent is about 19 times higher than the retardation factor obtained for the influent at pH 2 containing the same concentration of Pb (Table 4). This behavior is due to the high pH values of the efluent along the experiment at pH 5, as it can be seen in Fig. 3d, which promotes the Pb precipitation. Accordingly, Fig. 4 shows a higher retention at the bottom of the column where the influent is feed, for the tests at pH 5, implying a promptly high immobilization. In contrast, the effluent pH along

Table 4
Retardation factors determined for the tested metals and pH values.

C_0 (mg L^{-1})	Influent pH	R
47	2	27
	5	23
54	2	18
	5	339

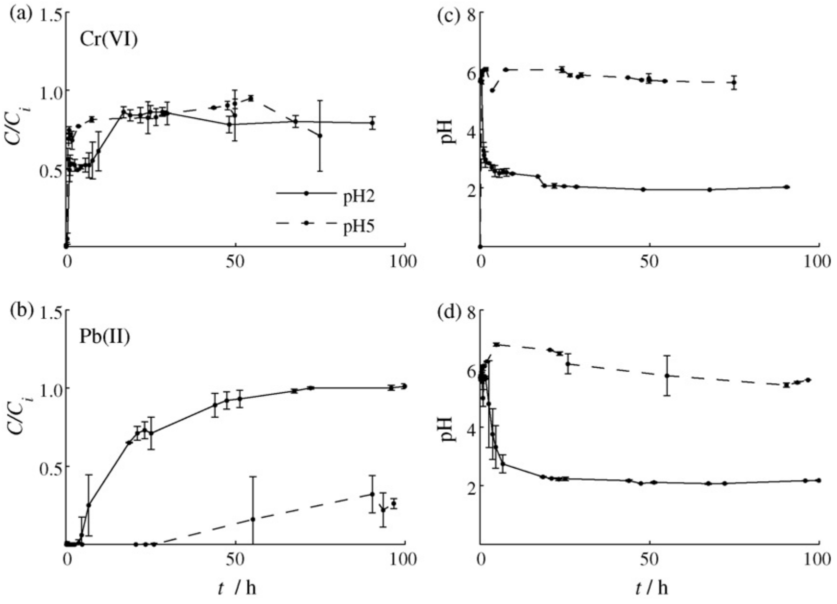

Fig. 3. (a) Effect of influent pH on the Cr(VI) breakthrough curves; (b) effect of influent pH on the Pb(II) breakthrough curves ($C_i \approx 50\,\mathrm{mg\,L^{-1}}$); (c) variation of the pH on Cr(VI) effluents (d) variation of the pH on Pb(II) effluents. The error bars depict the confidence interval for a level of confidence of 95%.

the experiment at pH 2 tends to decrease due to the already mentioned lower buffering capacity of the soil, avoiding precipitation phenomena.

4.4. FTIR spectral analysis

Fig. 5 shows the FTIR spectra of the soil samples of the bottom, centre and top of the columns bed after the sorption tests with the influent at pH 2 and of an uncontaminated soil sample. Clay minerals represented by the SiO–H stretch at $3695\,\mathrm{cm^{-1}}$, $3620\,\mathrm{cm^{-1}}$, Si–O–Si stretch at $1030\,\mathrm{cm^{-1}}$ and a small weak band at $694\,\mathrm{cm^{-1}}$ appear to play an important role in the sorption process of both metals, especially of Pb, since these bands tend to overlap for the contaminated samples [5,50,51]. In fact, heavy metals are sorbed by a variety of soil phases with hydroxyl groups on their surfaces and edges including the clay minerals, where sorption reactions are often more rapid.

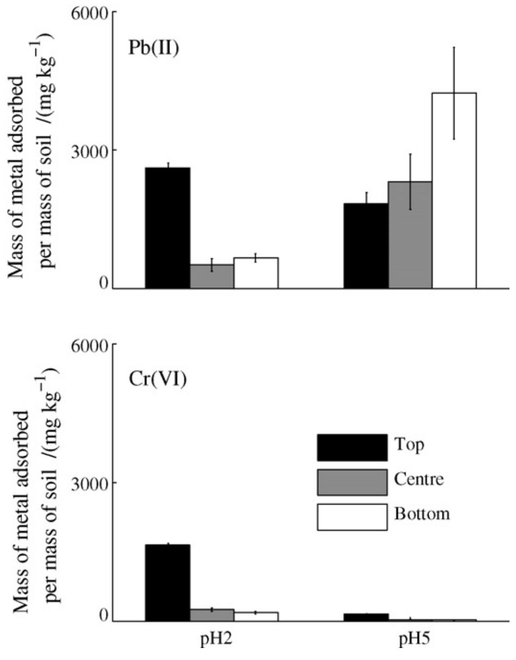

Fig. 4. Mass of metal retained per mass of soil in three different zones of the soil bed, for column test with Pb and Cr. The error bars depict the confidence interval for a level of confidence of 95%.

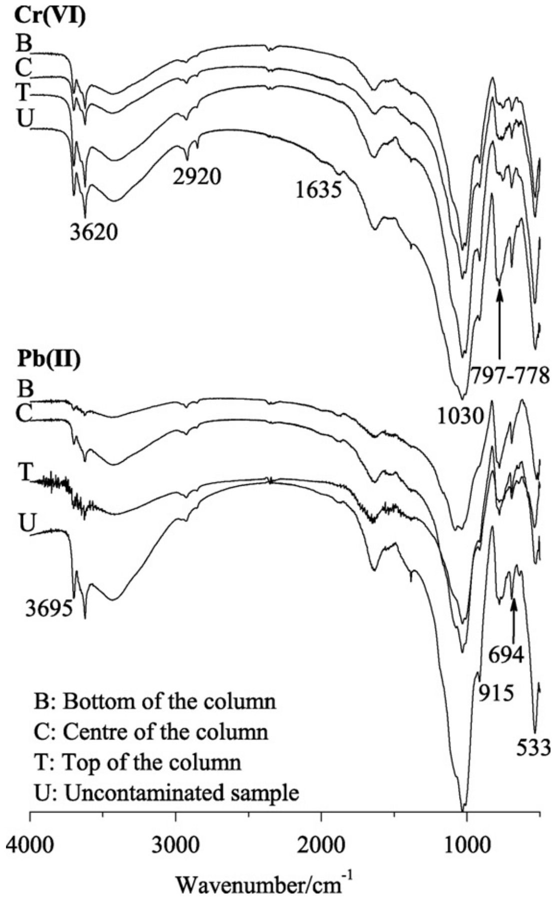

Fig. 5. FTIR spectra of column soil samples, before and after the flow experiments with Cr(VI) and Pb(II) influents at pH 2.

FTIR spectra of the soil used in Pb experiment shows a variation of O–H bend of adsorbed water (~1635 cm^{-1}), suggesting the formation of $PbOH^+$ in the surface. The soil sample contains some natural organic matter that greatly adsorbs trace metals resulting in the overlapping of the C–H stretch band (2920 cm^{-1}, 2850 cm^{-1}) in both spectrums. As already mentioned in previous sections, in the case of Cr this phenomenon can also result from the reduction of Cr(VI) to Cr(III) by natural organic matter [11,50,52,53].

5. Conclusions

The retention of Cr oxyanions and Pb cations onto a common loamy sand soil was studied at low different pH and high initial concentrations of the contaminating solutions. Despite the solution pH used in the batch tests, the cations of Pb are always rapidly retained in opposition to Cr whose sorption occurs slowly. The sorption kinetics of this ion is well described by the empirical power function and its rate constant increased with decreasing pH. The equilibrium studies showed that Pb adsorption was well described by the Langmuir monolayer theory and that Cr is retained mainly by physical adsorption described by Dubinin–Radushkevich model.

Finally, the continuous tests confirmed the high retention of Pb that increases with pH due to precipitation. It was also showed that Cr(VI) reduction, suggested by FTIR results, and the protonation of soil groups at low pH values are responsible for the higher retention of Cr onto soil. However, according to FTIR results, both metals adsorb mainly on the hydroxyl groups at the edge of the clay minerals.

In short, both metals have great mobility in acid environments threatening the quality of groundwater near industrial environments.

Acknowledgments

The authors gratefully acknowledge the financial support of this Project by the Fundação para a Ciência e Tecnologia, Ministério da Ciência e Tecnologia, Portugal (POCTI/CTA/44449/2002). They also acknowledge the PhD grant of Bruna Fonseca and the Pos-Doc grant of Cristina Quintelas.

References

[1] S. Serrano, F. Garrido, C.G. Campbell, M.T. Garcia-Gonzalez, Competitive sorption of cadmium and lead in acid soils of Central Spain, Geoderma 124 (2005) 91–104.

[2] P.K. Chaturvedi, C.S. Seth, V. Misra, Sorption kinetics and leachability of heavy metal from the contaminated soil amended with immobilizing agent (humus soil and hydroxyapatite), Chemosphere 64 (2006) 1109–1114.

[3] E.F. Covelo, M.L. Andrade, F.A. Vega, Heavy metal adsorption by humic umbrisols: selectivity sequences and competitive sorption kinetics, J. Colloid Interface Sci. 280 (2004) 1–8.

[4] A.R.A. Usman, The relative adsorption selectivities of Pb, Cu, Zn, Cd and Ni by soils developed on shale in New Valley, Egypt, Geoderma 144 (2008) 334–343.

[5] D.L. Sparks, Environmental Soil Chemistry, Academic Press, San Diego, 1995.

[6] C. Quintelas, E. Sousa, F. Silva, S. Neto, T. Tavares, Competitive biosorption of ortho-cresol, phenol, chlorophenol and chromium(VI) from aqueous solution by a bacterial biofilm supported on granular activated carbon, Process. Biochem. 41 (2006) 2087–2091.

[7] J. Jiang, R. Xu, Y. Wang, A. Zhao, The mechanism of chromate sorption by three variable charge soils, Chemosphere 71 (2008) 1469–1475.

[8] S.E. Fendorf, Surface reactions of chromium in soils and waters, Geoderma 67 (1995) 55–71.

[9] S.Z. Lee, L.Z. Chang, C.M. Chen, H.H. Yang, P.Y. Hu, The effect of hydration on adsorption and desorption of heavy metals in soils, J. Environ. Sci. Health, Part A 36 (2001) 63–74.

[10] M. Pantsar-Kallio, S.P. Reinikainen, M. Oksanen, Interactions of soil components and their effects on speciation of chromium in soils, Anal. Chim. Acta 439 (2001) 9–17.

[11] P.R. Wittbrodt, C.D. Palmer, Reduction of Cr(VI) in the presence of excess soil fulvic-acid, Environ. Sci. Technol. 29 (1995) 255–263.

[12] T. Narukawa, K.W. Riley, D.H. French, K. Chiba, Speciation of chromium in Australian fly ash, Talanta 73 (2007) 178–184.

[13] N. Martinez-Villegas, L.M. Flores-Velez, O. Dominguez, Sorption of lead in soil as a function of pH: a study case in Mexico, Chemosphere 57 (2004) 1537–1542.

[14] P. Srivastava, B. Singh, M. Angove, Competitive adsorption behavior of heavy metals on kaolinite, J. Colloid Interface Sci. 290 (2005) 28–38.

[15] F.J. Stevenson, M.A. Cole, Cycles of Soil, John Wiley & Sons Inc., New York, 1999.

[16] A.E. Barbosa, T. Hvitved-Jacobsen, Highway runoff and potential for removal of heavy metals in an infiltration pond in Portugal, Sci. Total Environ. 235 (1999) 151–159.

[17] H.B. Bradl, Adsorption of heavy metal ions on soils and soils constituents, J. Colloid Interface Sci. 277 (2004) 1–18.

[18] P.S. Hooda, B.J. Alloway, Cadmium and lead sorption behaviour of selected English and Indian soils, Geoderma 84 (1998) 121–134.

[19] T. Adhikari, M.V. Singh, Sorption characteristics of lead and cadmium in some soils of India, Geoderma 114 (2003) 81–92.

[20] J. Markiewiez-Patkowska, A. Hursthouse, H. Przybyla-Kij, The interaction of heavy metals with urban soils: sorption behaviour of Cd, Cu, Cr, Pb and Zn with a typical mixed brownfield deposit, Environ. Int. 31 (2005) 513–521.

[21] I. Yolcubal, N.H. Akyol, Retention and transport of hexavalent chromium in calcareous karst soils, Turk. J. Earth Sci. 16 (2007) 363–379.

[22] B. Fonseca, A. Teixeira, H. Figueiredo, T. Tavares, Modelling of the Cr(VI) transport in typical soils of the North of Portugal, J. Hazard. Mater. (2009), doi:10.1016/j.jhazmat.2009.01.049.

[23] K.G. Bhattacharyya, S. Sen Gupta, Adsorptive accumulation of Cd(II), Co(II), Cu(II), Pb(II), and Ni(II) from water on montmorillonite: influence of acid activation, J. Colloid Interface Sci. 310 (2007) 411–424.

[24] J.C. Echeverria, M.T. Morera, C. Mazkiaran, J.J. Garrido, Competitive sorption of heavy metal by soils. Isotherms and fractional factorial experiments, Environ. Pollut. 101 (1998) 275–284.

[25] Y.S. Ho, Review of second-order models for adsorption systems, J. Hazard. Mater. 136 (2006) 681–689.

[26] A. Gunay, E. Arslankaya, I. Tosun, Lead removal from aqueous solution by natural and pretreated clinoptilolite: adsorption equilibrium and kinetics, J. Hazard. Mater. 146 (2007) 362–371.

[27] H. Freundlich, Concerning adsorption in solutions, Z. Phys. Chem. – Stochiometrie Verwandtschaftslehre 57 (1906) 385–470.

[28] I. Langmuir, The adsorption of gases on plane surfaces of glass, mica and platinum, J. Am. Chem. Soc. 40 (1918) 1361–1403.

[29] M.M. Dubinin, The potential theory of adsorption of gases and vapors for adsorbents with energetically nonuniform surfaces, Chem. Rev. 60 (1960) 235–241.

[30] T.V.N. Padmesh, K. Vijayaraghavan, G. Sekaran, M. Velan, Application of two- and three-parameter isotherm models: biosorption of Acid Red 88 onto *Azolla microphylla*, Biorem. J. 10 (2006) 37–44.

[31] A. Sarl, M. Tuzen, Biosorption of cadmium(II) from aqueous solution by red algae (*Ceramium virgatum*): equilibrium, kinetic and thermodynamic studies, J. Hazard. Mater. 157 (2008) 448–454.

[32] V. Srihari, A. Das, Comparative studies on adsorptive removal of phenol by three agro-based carbons: equilibrium and isotherm studies, Ecotoxicol. Environ. Saf. 71 (2008) 274–283.

[33] Z. Aksu, Determination of the equilibrium, kinetic and thermodynamic parameters of the batch biosorption of nickel(II) ions onto *Chlorella vulgaris*, Process. Biochem. 38 (2002) 89–99.

[34] A.R. Khan, R. Ataullah, A. AlHaddad, Equilibrium adsorption studies of some aromatic pollutants from dilute aqueous solutions on activated carbon at different temperatures, J. Colloid Interface Sci. 194 (1997) 154–165.

[35] R. Sips, On the structure of a catalyst surface, J. Chem. Phys. 16 (1948) 490–495.

[36] J. Toth, State equations of solid–gas interface layers, Acta Chim. Acad. Sci. Hung. 69 (1971) 311–328.

[37] USEPA, Microwave Assisted Acid Digestion of Sediments, Sludges, Soils, and Oils, Environmental Protection Agency, United States of America, 3051, 2007.

[38] W.H. Hendershot, H. Lalande, M. Duquette, Ion exchange and exchangeable cations, in: M.R. Carter, E.G. Gregorich (Eds.), Soil Sampling and Methods of Analysis, 1993, pp. 197–206.

[39] A. Mehlich, Rapid determination of cation and anion exchange properties and pH of soils, J. Assoc. Off. Anal. Chem. 36 (1953) 445–457.

[40] J. Tinsley, The determination of organic carbon in soils by dichromate mixture, IV Int. Cong. Soil Sci. (1950) 161–164.

[41] J.P. Chen, L. Wang, Characterization of metal adsorption kinetic properties in batch and fixed-bed reactors, Chemosphere 54 (2004) 397–404.

[42] C.A. Impellitteri, H.E. Allen, Y. Yin, S. You, J.K. Saxe, in: H.M. Selim, D.L. Sparks (Eds.), Heavy Metals Release in Soils, Lewis Publisher, Boca Raton, 2001, pp. 149–165.

[43] H. Teng, C.T. Hsieh, Activation energy for oxygen chemisorption oil carbon at low temperatures, Ind. Eng. Chem. Res. 38 (1999) 292–297.

[44] D.G. Strawn, D.L. Sparks, Effects of soil organic matter on the kinetics and mechanisms of Pb(II) sorption and desorption in soil, Soil Sci. Soc. Am. J. 64 (2000) 144–156.

[45] C.L. Liu, T.W. Chang, M.K. Wang, C.H. Huang, Transport of cadmium, nickel, and zinc in Taoyuan red soil using one-dimensional convective-dispersive model 1, Geoderma 131 (2006) 181–189.

[46] D.C. Ghosh, R. Biswas, Theoretical calculation of absolute radii of atoms and ions. Part 2. The ionic radii, Int. J. Mol. Sci. 4 (2003) 379–407.

[47] Z. Bekci, Y. Seki, M.K. Yurdakoc, Equilibrium studies for trimethoprim adsorption on montmorillonite KSF, J. Hazard. Mater. 133 (2006) 233–242.

[48] P.H. Connett, K.E. Wetterhahn, Reaction of chromium(VI) with thiols—pH-dependence of chromium(VI) thio ester formation, J. Am. Chem. Soc. 108 (1986) 1842–1847.

[49] L.D. Anderson, D.B. Kent, J.A. Davis, Batch experiments characterizing the Reduction of Cr(VI) using suboxic material from a mildly reducing sand and gravel aquifer, Environ. Sci. Technol. 28 (1994) 178–185.

[50] R.A. Alvarez-Puebla, C. Valenzuela-Calahorro, J.J. Garrido, Modeling the adsorption and precipitation processes of Cu(II) on humin, J. Colloid Interface Sci. 277 (2004) 55–61.

[51] E. Smidt, K. Meissl, The applicability of Fourier transform infrared (FT-IR) spectroscopy in waste management, Waste Manage. 27 (2007) 268–276.

[52] P.M. Jardine, S.E. Fendorf, M.A. Mayes, I.L. Larsen, S.C. Brooks, W.B. Bailey, Fate and transport of hexavalent chromium in undisturbed heterogeneous soil, Environ. Sci. Technol. 33 (1999) 2939–2944.

[53] M.K. Banks, A.P. Schwab, C. Henderson, Leaching and reduction of chromium in soil as affected by soil organic content and plants, Chemosphere 62 (2006) 255–264.